ISSN NO. 2320-5407

*Journal homepage: http://www.journalijar.com*

*INTERNATIONAL JOURNAL OF ADVANCED RESEARCH*

**RESEARCH ARTICLE**

# Performance and Theoretical Study on Corrosion Inhibition of 304 SS in Hydrochloric Acid Solutions by Chalcone Compounds

*** A.S.Fouda[1], A.M.Eldesoky[2], A.F.Hassan[3] and A.Abdelhakim[1]**

**1.** Department of Chemistry, Faculty of Science, El-Mansoura University, El-Mansoura-35516, Egypt
**2.** Engineering Chemistry Department, High Institute of Engineering &Technolog ( New Damietta), Egypt and Chemistry Department, Qunfudah University College, Umm Al-Qura University, KSA
**3.** Department of Chemistry, Faculty of Science, Damanhour University, Damanhour, Egypt

## *Manuscript Info*

***Manuscript History:***

Received: 11 January 2014
Final Accepted: 26 February 2014
Published Online: March 2014

***Key words:***
Corrosion inhibition, SS type 304, HCl, Chalcone compounds, SEM, EDX

***Corresponding Author***

**A.S.Fouda**

## *Abstract*

Inhibition performance of two derivatives of chalcone compounds against corrosion of SS type 304 in 1 M HCl was investigated by weight loss and electrochemical measurements. The inhibition efficiency increased with increasing inhibitor's concentration, but decreased with the increase in temperature and concentration of the acid. The results indicated that these compounds act as mixed type inhibitors and are adsorbed on 304 SS surface following Langmuir adsorption isotherm. The theoretical results revealed that the binding energy between compound (1) molecule and iron surface is the highest among the two studied compounds. The morphology of inhibited 304 SS was analyzed by scanning electron microscope (SEM) technology with energy dispersive X-ray spectroscopy (EDX).



## l. Introduction

Acid solutions are, especially hydrochloric acid, widely used in various industrial processes such as oil well acidification, the petrochemical processes, acid pickling and acidic cleaning [1–3], which generally leads to serious metallic corrosion. As the most effective and economic method, inhibitors are applied in these acid solutions to control the metal dissolution [4,5]. There is a considerable amount of effort devoted to inhibitors. Organic compounds usually serve as inhibitors, and generally protect the metal from corrosion by forming a protection film on the metal surface [6]. Most of the well-known organic inhibitors are the compounds containing nitrogen, sulfur, oxygen atoms and p-bonds [7]. Those structures with the polar groups, which can act as the reactive centers, play an important role in the adsorption of inhibitor molecules on the metal surface. Benzimidazole and its derivatives have received considerable attention on their inhibition properties for metallic corrosion over the past years [8–10]. Benzimidazole is a heterocyclic organic compound, and the nitrogen atom and the aromatic ring in molecular structure are likely to facilitate the adsorption of the compounds on the metal surface [11]. Some derivatives of benzimidazole have been demonstrated as excellent inhibitors for metals and alloys in acidic solution, and exhibit different inhibition performance with the difference in substituent groups and substituent positions on the imidazole ring [12–18].The efficiency of organic inhibitors depends on their structure, especially chemical/electronic structure. Those structural parameters can be obtained from quantum chemical methods, which have been extensively used to study reaction mechanism. Several groups [19–23] have studied the inhibition mechanism of some organic molecules by quantum chemical calculations, and a nonlinear model based on multiple regressions has successfully been established to probe the relationship between the quantum chemical parameters of inhibitor molecule and inhibition efficiency [24–26]. For quantum chemical study, however, it is difficult to give the information on the interaction between metal surface and inhibitor molecule, which is essential to understand the inhibition performance of inhibitors. In recent years, the molecular dynamics (MD) simulations have been used to study the interaction between inhibitors and metal surface. MD simulations can illustrate the adsorption of the molecules onto the corroding metal surface at molecular level, and present the conformation of organic molecule adsorbed onto metal surface and the interaction

energy between inhibitor and metal surface [27–31]. Therefore, molecular dynamics simulations provide insights into the design of inhibitor systems with superior properties, and the interaction energy between organic molecule and metal surface can explain the difference in inhibition efficiency between different organic inhibitors [32–34].
In this paper, the corrosion inhibition performance of chalcone compounds for 304 SS in hydrochloric acid solutions was investigated by weight loss and electrochemical techniques. PM3 calculations were performed to study the electronic structure and the adsorption of chalcone compounds onto SS. SEM and EDX examination of the 304SS in 1 M HCl surface revealed that these compounds prevented 304SS corrosion by adsorption on its surface to form a protective film and acts as a barrier to corrosive media

## 2. Experimental Methods

### 2.1. Materials

All chemicals and reagents used are with analytical grade and used without further purification.

### 2.2. Solutions

The aggressive solutions used were made of AR grade HCl. Appropriate concentrations of acid were prepared using bidistilled water. $10^{-3}$M stock solutions from the investigated compounds were prepared by dissolving the appropriate weights of the used chemically pure solid compounds in ethanol. Various concentrations ($1 \times 10^{-6}$- $25 \times 10^{-6}$ M) of inhibitors were obtained by dilution with bidistilled water.

### 2.3. Weight loss method

Seven parallel stainless steel sheets of 2 x 2 x 0.2 cm were abraded with emery paper upto 1200 grit, washed with bidistilled water and acetone. After weighing accurately, the specimens were immersed in 100 ml beaker, which contained 100 ml 1 M HCl with and without addition of different concentrations of inhibitors at 25±1°C. The test specimens were suspended by suitable glass hooks at the edge of the basin, and under the surface of the test solution by about 1cm. All the aggressive acid solutions were open to air. After specified immersion time, the specimens were taken out, washed, dried, and weighed. The average weight loss of the three parallel stainless steel sheets could be obtained. Then the tests were prepared at different temperatures. The inhibition efficiency (% IE) and the degree of surface coverage (θ) of investigated inhibitors on the corrosion of stainless steels were calculated from the following equation [35]:

$$\% IE = \theta \times 100 = [(W_o - W)/ W_o] \times 100 \quad (1)$$

where $W_o$ and W are the values of the average weight losses without and with addition of the inhibitor, respectively.

### 2.4. Potentiodnamic polarization measurements

Polarization experiments were carried out in a conventional three-electrode cell with a platinum counter electrode and a saturated calomel electrode (SCE) coupled to a fine Luggin capillary as the reference electrode. The working electrode was in the form of a square cut from stainless steel sheet (1 x 1 cm) embedded in epoxy resin of polytetrafluoroethelene so that the flat surface was the only surface in the electrode. Before polarization scanning, working electrode was immersed in the test electrolyte of 100 ml in volume for 30 min. until steady state and the open circuit potential (OCP) was attained which was taken as $E_{OC}$. All experiments were carried out at 25 ±1°C using Lab companion circulator thermostat and solutions were not deaerated. For polarization measurements potential from -350 to 100 mV (relative to open circuit potential, $E_{OC}$) was applied. % IE and the degree of surface coverage (θ) were calculated from the following equation:

$$\% IE = \theta \times 100 = [(i_{corr} - i_{corr(inh)}) / i_{corr}] \times 100 \quad (2)$$

where $i_{corr}$ and $i_{corr(inh)}$ are the uninhibited and inhibited corrosion current density values, respectively, determined by extrapolation of Tafel lines to the corrosion potential.

### 2.5. Electrochemical impedance spectroscopy method

The EIS spectra were recorded at open circuit potential (OCP) after immersion the electrode for 10 minutes in the test solution. The AC signal was 5 mV peak to peak and the frequency range studied was between 100 kHz and 0.2 Hz. The inhibition efficiency (% IE) and the surface coverage (θ) of the used inhibitors obtained from the impedance measurements can be calculated by applying the following relation:

$$\% IE = \theta \times 100 = [1-(R^{\circ}_{ct}/R_{ct})] \times 100 \quad (3)$$

where $R^{o}_{ct}$ and $R_{ct}$ are the charge transfer resistance in the absence and presence of inhibitor, respectively.

### 2.6. Electrochemical Frequency Modulation Technique

EFM experiments were performed with applying potential perturbation signal with amplitude 10 mV with two sine waves of 2 and 5 Hz. The choice for the frequencies of 2 and 5Hz was based on three arguments [36]. The larger

peaks were used to calculate the corrosion current density ($i_{corr}$), the Tafel slopes ($\beta_c$ and $\beta_a$) and the causality factors CF2 and CF3 [37].

All electrochemical experiments were carried out using Gamry instrument PCI300/4 Potentiostat/Galvanostat/Zra analyzer, DC105 corrosion software for polarization, EIS300 software for electrochemical impedance spectroscopy software, EFM140 software for electrochemical frequency modulation and Echem Analyst 5.5 for results plotting, graphing, data fitting and calculating.

**2.7. SEM-EDX Measurement**

The 304 stainless steel surfaces was prepared by keeping the specimens for 3days in 1 M HCl in presence and absence of optimum concentration of chalcone compounds, after abraded mechanically using different emery papers up to 1200 grit size. Then, after this immersion time, the specimens were washed gently with bidistilled water, carefully dried and mounted into the spectrometer without any further treatment.

The corroded alloy surfaces were examined using an X-ray diffractometer Philips (pw-1390) with Cu-tube (Cu Ka1, l = 1.54051 A °), a scanning electron microscope (SEM, JOEL, JSM-T20, Japan).

*2.8. Theoretical study*

Accelrys (Material Studio Version 4.4) software for quantum chemical calculations has been used.

**2.9. Inhibitors**

## 3. Results and discussion

**3.1. Weight loss measurements**

The weight losses of 304 stainless steel specimens in 1 M HCl solution, without and with different concentrations from the investigated inhibitors, were determined at different times of immersion at 25°C. Figure (1) represents the weight loss of 304 stainless steel in1 M HCl solution, without and with different concentrations of compound (1) as an example. Similar curves were obtained for compound (2) (not shown). The presence of inhibitors reduces the corrosion rate of steel in HCl. Values of % IE are tabulated in Table (3). In all cases, the increase in the inhibitor concentration was accompanied by a decrease in the weight loss and an increase in % IE. These results lead to the conclusion that, these compounds under investigation are fairly efficient as inhibitors for SS type 304 dissolution in HCl solution. Careful inspection of these results showed that, at the same inhibitor concentration, the ranking of the inhibitors according to % IE is as follow: compound (1) > compound (2)

**The experiments were performed with 304 SS specimens in the form of rods and sheets with the following composition in Table (1):**

| Stainless steel type | Composition (weight %) | | | | | | | | |
|---|---|---|---|---|---|---|---|---|---|
| | C | Mn | P | S | Si | Cr | Ni | Mo | Fe |
| 304 | 0.08 | 2.0 | 0.04 | 0.03 | 0.75 | 18-20 | 8-11 | --- | rest |

**Table (2): Chemical structures, names, molecular formulas and molecular weights of chalcone compounds** [38]

| Comp | Structures | Names | Mol. Weights / Mol. Formulas |
|---|---|---|---|
| 1 | 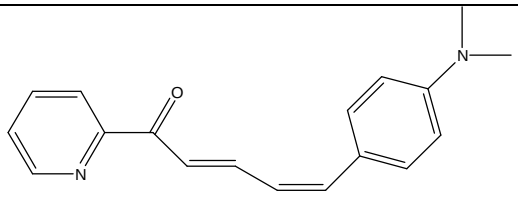 | (2 E,4 Z)-5-(4-dimethyl amino) Phenyl)-1-(pyridin-2-yl )penta-2,4-dien-1-one | $C_{18}H_{18}N_2O$ 278.35 |

| | | | |
|---|---|---|---|
| 2 | 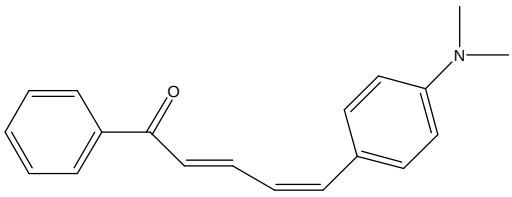 | (2 E,4 Z)-5-(4-dimethyl amino) Phenyl)-1-phenyl penta-2,4-dien-1-one | $C_{19}H_{19}NO$ 277.36 |

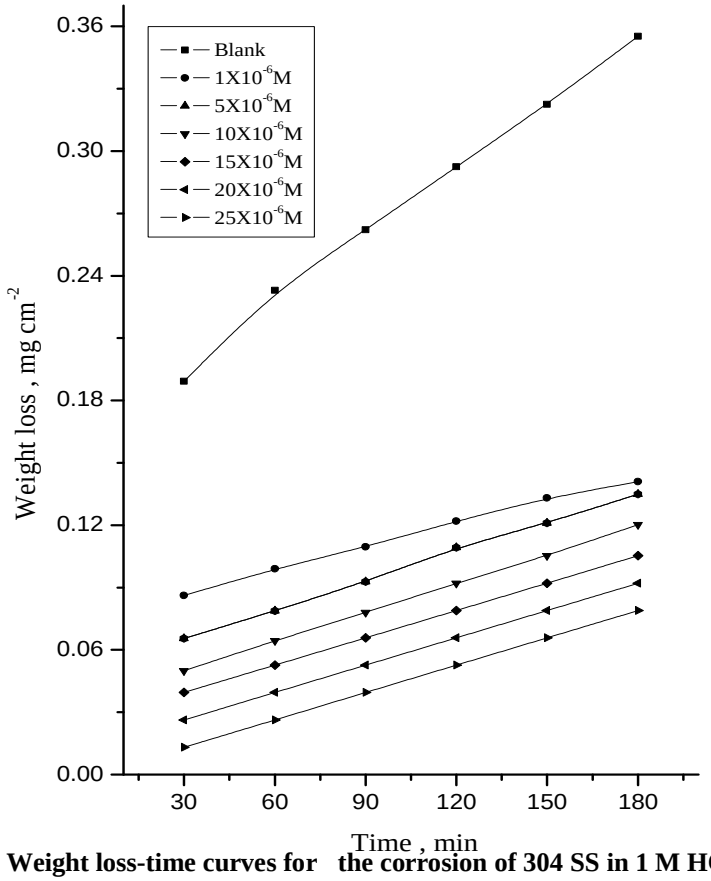


**Figure. (1): Weight loss-time curves for the corrosion of 304 SS in 1 M HCl in the absence and presence of different concentrations of compound (1) at 25°C**

**Table (3): Variation of inhibition efficiency (% IE) of different compounds with their molar concentrations from weight loss measurements at 120 min immersion in 1 M HCl at 25°C**

| Conc., M | inhibition efficiency (% IE) | |
|---|---|---|
| | (1) | (2) |
| 1 x $10^{-6}$ | 58.3 | 54.6 |
| 5 x $10^{-6}$ | 62.6 | 59.3 |
| 10 x $10^{-6}$ | 68.5 | 65.3 |
| 15 x $10^{-6}$ | 73.0 | 70.3 |
| 20 x $10^{-6}$ | 77.5 | 73.7 |
| 25 x $10^{-6}$ | 82.0 | 77.9 |

### 3.1.1- Adsorption isotherm

One of the most convenient ways of expressing adsorption quantitatively is by deriving the adsorption isotherm that characterizes the metal/inhibitor/ environment system [39].Various adsorption isotherms were applied to fit θ values but the best fit was found to obey Langmuir adsorption isotherm which may be expressed by [40]:

$C/\theta = 1/K_{ads} + C$ (4)

where C is inhibitor concentration and K is equilibrium constant of adsorption. It is well known that the standard adsorption free energy ($\Delta G°_{ads}$) is related to equilibrium constant of adsorption (K) by the following equation [41]:

$K_{ads} = 1/55.5 \exp [-\Delta G°_{ads}/RT]$ (5)

Figures (2,3) represents the plot of (C/θ) against C for two investigated compounds for the corrosion of stainless steel type 304 in 1M HCl at 25°C. As can be seen from Figs (2, 3) the Langmuir isotherm is the best one which explains the experimental results. The values of $K_{ads}$ and $\Delta G°_{ads}$ calculated by Langmuir isotherm are given in Table (4). The negative values of $\Delta G°_{ads}$ suggested that the adsorption of inhibitors molecules onto steel surface is a spontaneous process. The magnitude of adsorption heat reaches the magnitude of chemical reaction heat, which is the result of the transference of electron from donating atoms in the inhibitor molecule to the d-orbital of the iron atom. This means that the given inhibitor molecules will form monolayer on the steel surface. In general the values of $\Delta G°_{ads}$ obtained from Langmuir isotherms and the adsorption of inhibitors decreases in the order: compound (1) > compound (2).

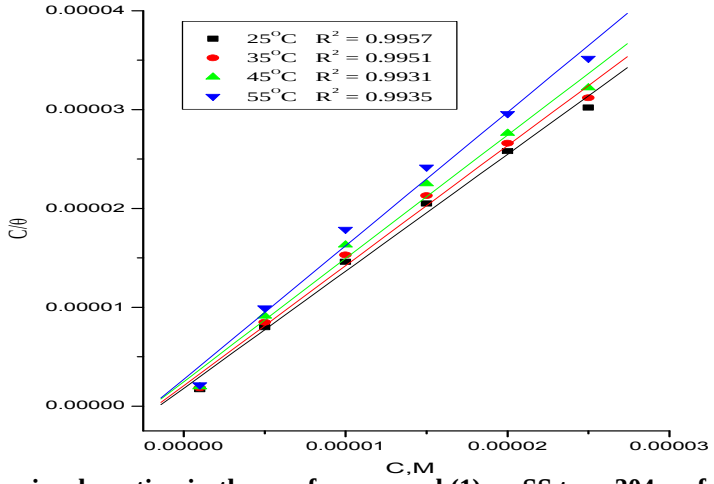


**Figure (2): Langmuir adsorption isotherm of compound (1) on SS type 304 surface in 1 M HCl at different temperatures**

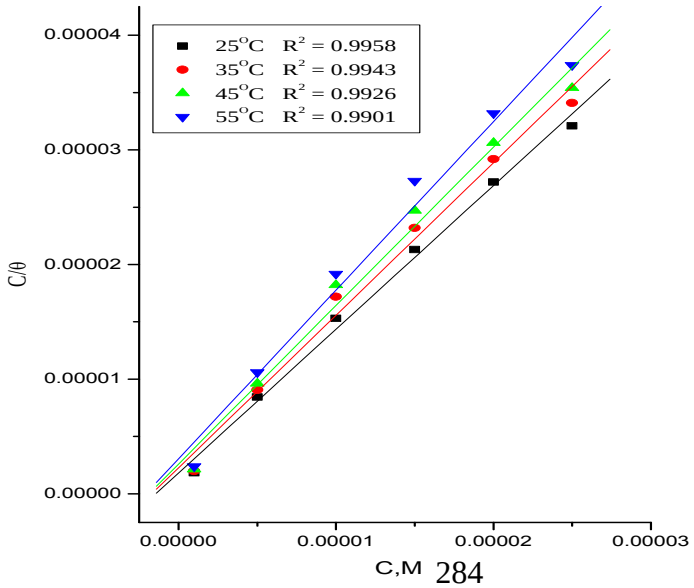

**Figure (3): Langmuir adsorption isotherm of compound (2) on SS type 304 surface in 1 M HCl at different temperatures**

### 3.1.2. Thermodynamic adsorption parameters

The well-known thermodynamic adsorption parameters are the free energy of adsorption ($\Delta G°_{ads}$), the heat of adsorption ($\Delta H°_{ads}$) and the entropy of adsorption ($\Delta S°_{ads}$).These quantities can be calculated by various mathematical methods depending on the estimated values of $k_{ads}$. From adsorption isotherm, at different temperatures as follows:

The $\Delta G°_{ads}$ values at all studied temperatures can be calculated from the following equation:

$$K_{ads} = (1/ 55.5) \exp (-\Delta G°_{ads}/ RT) \quad (6)$$

where 55.5 is the concentration of water in ($M^{-1}$) at metal\solution interface. The heat of adsorption ($\Delta H°_{ads}$) could be calculated according to the Van't Hoff equation:

$$\text{Log}K_{ads} = (- \Delta H°_{ads} / 2.303RT) + \text{constant} \quad (7)$$

In order to calculate heat of adsorption ($\Delta H°_{ads}$), log $K_{ads}$ was plotted against 1/T as shown in Figs (2,3). The straight lines were obtained with slope equal to ($-\Delta H°_{ads}/R$). Then in accordance with the basic equation:

$$\Delta G°_{ads} = \Delta H°_{ads} - T\Delta S°_{ads} \quad (8)$$

By introducing the obtained $\Delta G°_{ads}$ and $\Delta H°_{ads}$ values in equation (8), the entropy of adsorption ($\Delta S°_{ads}$) values were calculated at all studied temperatures. All estimated thermodynamic adsorption parameters for the studied compounds on SS type 304 from 1 M HCl solution were listed in Table (4). Inspection of the obtained data, it was found that: The negative values of $\Delta G°_{ads}$ reflect that the adsorption of studied inhibitors on 304SS surface from 1 M HCl solution is spontaneous process. $\Delta G°_{ads}$ values increase (become less negative) with an increase of temperature which indicates the occurrence of exothermic process at which adsorption was unfavorable with increasing reaction temperature as the result of the inhibitor desorption from the 304SS surface. It is usually accepted that the value of $\Delta G°_{ads}$ around 20 kJ mol-1 or lower indicates the electrostatic interaction between charged metal surface and charged organic molecules in the bulk of the solution while those around -40 kJ mol-1 or higher involve charge sharing or charge transfer between the metal surface and organic molecules. From the obtained values of $\Delta G°_{ads}$ it was found the existence of comprehensive (physical and chemical adsorption).

The negative sign of $\Delta H°_{ads}$ reveals that the adsorption of inhibitor molecules is an exothermic process. Generally, an exothermic adsorption process suggests either physisorption or chemisorption while endothermic process is attributed to chemisorption. The unshared electron pairs in investigated molecules may interact with d-orbitals of 304SS to provide a protective chemisorbed film. In the case of investigated compounds, the absolute values of enthalpy are relatively low, approaching those typical of physisorption. The values of $\Delta S°_{ads}$ in the presence of inhibitors are large and negative that is accompanied with exothermic adsorption process.

**Table (4): Thermodynamic parameters for the adsorption of Chalcone compounds on 304SS surface in 1 M HCl at different temperatures**

| Comp. | Temperature, °C | $-\Delta G°_{ads}$, kJ mole $^{-1}$ | $-\Delta H°_{ads}$, kJ mol$^{-1}$ | $-\Delta S°_{ads}$ J mol$^{-1}$ k$^{-1}$ | $K_{ads}$, $M^{-1}x10^{-4}$ |
|---|---|---|---|---|---|
| 1 | 25 | 45.9 | 11.4 | 105.1 | 55.3 |
| | 35 | 44.7 | | 105.2 | 48.3 |
| | 45 | 43.8 | | 104.9 | 40.4 |
| | 55 | 42.7 | | 105.2 | 36.8 |
| 2 | 25 | 45.6 | 13.9 | 96.7 | 55.0 |
| | 35 | 44.6 | | 96.4 | 44.3 |
| | 45 | 43.6 | | 96.6 | 38.5 |
| | 55 | 42.7 | | 96.6 | 32.7 |

### 3.1.2- Effect of temperature

The effect of temperature on the inhibited acid-metal reaction is highly complex, because many changes occur on the metal surface, such as rapid etching and desorption of the inhibitor and the

Generally the corrosion rate increases with the rise of temperature. It was found that the inhibition efficiency decreases with increasing temperature and increases with increasing the concentration of the inhibitor. The activation energy ($E^*_a$) of the corrosion process was calculated using Arrhenius equation [42]:

$k_{corr} = A \exp(-E^*_a / RT)$ (9)

where $k_{corr}$ corrosion rate, A is Arrhenius constant, R is the gas constant and T is the absolute temperature. The values of activation energies $E^*_a$ can be obtained from the slope of the straight lines of plotting log $k_{corr}$ vs. 1/T in the presence and absence of investigated compounds at various temperatures Figure (4) and are given in Table (5), it is noted that the values of activation energy increase in the presence of inhibitors and with increase of the concentration of the inhibitors. This is due to the presence of a film of inhibitors on 304 SS surface. The activation energy for the corrosion of 304SS in 1 M HCl was found to be 50.4 kJ $mol^{-1}$ which is in good agreement with the work carried out by others [43-44]An alternative formulation of the Arrhenius equation is the transition state equation 10 [45]:

$k_{corr} = RT/Nh \exp(\Delta S^*/R) \exp(-\Delta H^*/RT)$ (10)

where h is Planck's constant, N is Avogadro's number, $\Delta S^*$ is the entropy of activation and $\Delta H^*$ is the enthalpy of activation. Figure (5) shows a plot of log ($k_{corr}$ / T) vs. (1/T). Straight lines are obtained with a slope of ($\Delta H^*/2.303$ R) and an intercept of (log R/Nh + $\Delta S^*/2.303$ R) from which the values of $\Delta H^*$ and $\Delta S^*$ are calculated and also listed in Table (5). From inspection of Table (5) it is clear that the positive values of $\Delta H^*$ reflect that the process of adsorption of the inhibitors on the 304 SS surface is an endothermic process; it is attributable unequivocally to chemisorption. Typically, the enthalpy of a chemisorption process approaches 100 kJ mol-1 [46]. More interesting behavior was observed in Table (5) that positive ΔS* values is accompanied with endothermic adsorption process. This is agrees with what expected, when the adsorption is an endothermic process, it must be accompanied by an increase in the entropy change and vies versa [47].It is seen that investigated derivatives have inhibiting properties at all the studied temperatures and the values of % IE decrease with temperature increase. This shows that the inhibitor has experienced a significant decrease in its protective properties with increase in temperature. This decrease in the protective properties of the inhibitor with increase in temperature may be connected with two effects; a certain drawing of the adsorption-desorption equilibrium towards desorption (meaning that the strength of adsorption process decreases at higher temperatures) and roughening of the metal surface which results from enhanced corrosion. These results suggest that physical adsorption may be the type of adsorption of the inhibitor on the 304 SS surface.

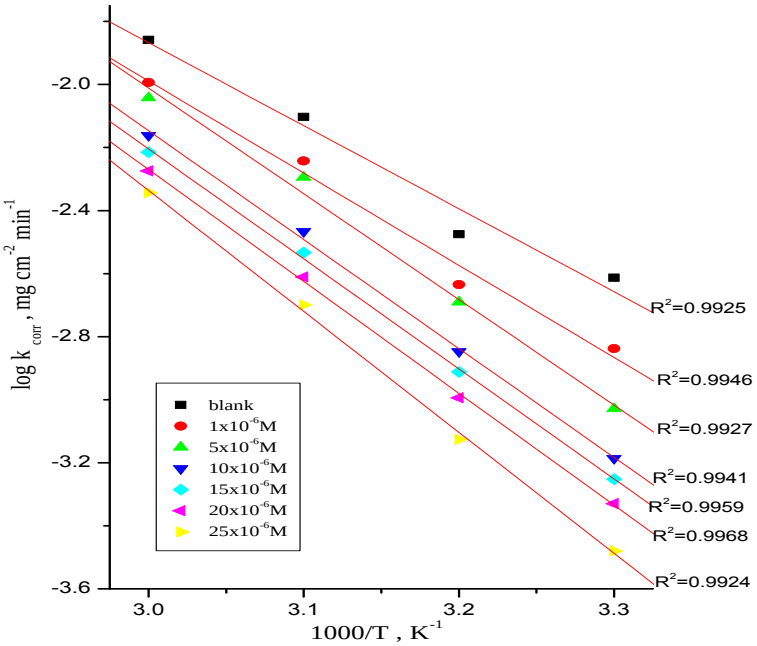


**Figure (4): Arrhenius plots for 304SS corrosion rates ($k_{corr}$) after 120 minutes of immersion in 1 M HCl in the absence and presence of different concentrations of compound (1)**

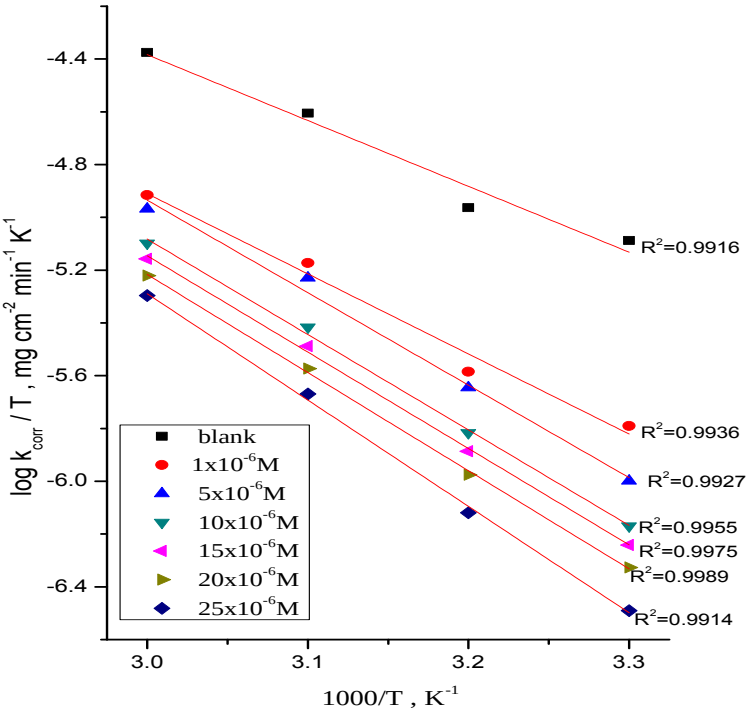


**Figure (5): Plots of (log $k_{corr}$/T)vs.1/T for corrosion of 304SS in 1M HCl in the absence and presence of different concentrations of compound (1)**

**Table (5): Activation parameters for the dissolution of 304SS in the presence and absence of different concentrations of different compounds in 1 M HCl**

| Inhibitor | Conc.,x $10^{-6}$ M | Activation parameters | | |
|---|---|---|---|---|
| | | $E_a^*$ | $\Delta H^*$ | $-\Delta S^*$ |
| | | kJ $mol^{-1}$ | kJ $mol^{-1}$ | J $mol^{-1}$ $K^{-1}$ |
| Free Acid 1M HCl | 0 | 50.4 | 20.2 | 139.6 |
| 1 | 1 | 59.5 | 24.6 | 118.8 |
| | 5 | 68.5 | 28.5 | 92.0 |
| | 10 | 70.5 | 29.4 | 88.7 |
| | 15 | 71.2 | 29.7 | 88.0 |
| | 20 | 72.4 | 30.2 | 85.6 |
| | 25 | 78.2 | 32.7 | 69.3 |
| 2 | 1 | 50.4 | 23.0 | 121.5 |
| | 5 | 54.6 | 26.4 | 97.4 |
| | 10 | 62.8 | 28.0 | 87.4 |
| | 15 | 64. 7 | 28.2 | 86.5 |
| | 20 | 65.3 | 28.5 | 91.4 |
| | 25 | 66.4 | 29.4 | 82.5 |

### 3.2. Potentiodynamic polarization

Anodic and cathodic polarizations were carried out potentiodynamic in unstirred 1 M HCl solutionin the absence

and presence of various concentrations of the inhibitors at 25°C over potential range 300 mV ± OCP. The results are represented in Figure. (6) for compound (1), similar behaviors were obtained for other compound. The obtained potentiodynamic polarization parameters are given in Table (6). These results indicate that the cathodic and anodic curves obtained exhibit Tafel-type behavior. Additionally, the form of these curves is very similar either in the cathodic or in the anodic side, which indicates that the mechanisms of 304SS dissolution and hydrogen reduction apparently remain unaltered in the presence of these additives. Addition of chalcone compounds decreased both the cathodic and anodic current densities and caused mainly parallel displacement to the more negative and positive values, respectively, i.e. the presence of organic derivatives in solution inhibits both the hydrogen evolution and the anodic dissolution processes with overall shift of $E_{corr}$ to more negative values with respect to the OCP.

The results also show that the slopes of the anodic and the cathodic Tafel slopes ($\beta_a$ and $\beta_c$) were slightly changed on increasing the concentration of the tested compounds. This indicates that there is no change of the mechanism of inhibition in presence and absence of inhibitors. The fact that the values of $\beta_c$ are slightly higher than the values of $\beta_a$ suggesting a cathodic action of the inhibitor. This could be interpreted as an action of mixed inhibitor control over the electrochemical semi-reactions. This means that the chalcone derivatives are mixed type inhibitors, but the cathode is more preferentially polarized than the anode. The higher values of Tafel slope can be attributed to surface kinetic process rather the diffusion-controlled process [48]. The constancy and the parallel of cathodic slope obtained from the electrochemical measurements indicate that the hydrogen evolution reaction was activation controlled [49] and the addition of these derivatives did not modify the mechanism of this process. This result suggests that the inhibition mode of the organic derivatives used was by simple blockage of the surface by adsorption.

**Figure (6): Potentiodynamic polarization curves for the corrosion of 304SS in 1 M HCl in the absence and presence of various concentrations of compound (1) at 25°C**

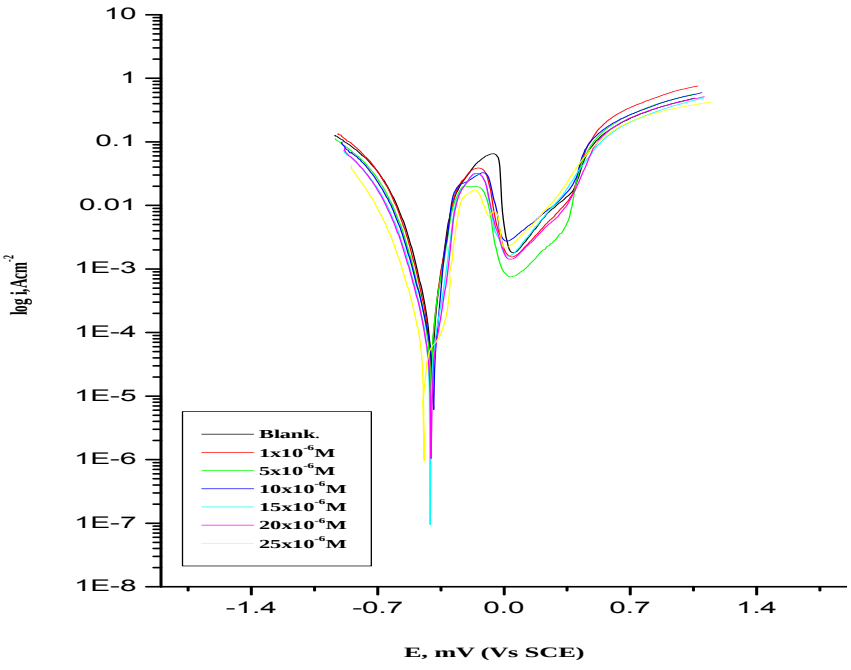

**Table (6): The effect of concentration of the investigated compounds on the free corrosion potential ($E_{corr}$), corrosion current density ($i_{corr}$), Tafel slopes ($\beta_a$& $\beta_c$), degree of surface coverage (θ), and inhibition efficiency (% IE) for the corrosion of 304SS in 1 M HCl at 25°C**

| Comp | Conc., $x10^{-6}$M | $-E_{corr.}$, mVvs SCE | $i_{corr}$, μA $cm^{-2}$ | $\beta_a$, mV $dec^{-1}$ | $\beta_c$ , mV $dec^{-1}$ | θ | % IE |
|---|---|---|---|---|---|---|---|
| | Blank | 399 | 221.0 | 94 | 133 | ---- | ----- |
| 1 | 1 | 405 | 104.0 | 64 | 106 | 0.529 | 52.9 |
| | 5 | 442 | 89.00 | 60 | 126 | 0.597 | 59.7 |
| | 10 | 404 | 75.60 | 55 | 88 | 0.658 | 65.8 |
| | 15 | 391 | 62.50 | 46 | 107 | 0.717 | 71.7 |
| | 20 | 408 | 53.50 | 68 | 108 | 0.758 | 75.8 |
| | 25 | 404 | 39.30 | 66 | 103 | 0.819 | 81.9 |
| 2 | 1 | 403 | 113.0 | 82 | 133 | 0.489 | 48.9 |
| | 5 | 391 | 103.0 | 48 | 91 | 0.534 | 53.4 |
| | 10 | 420 | 82.9 | 39 | 124 | 0.625 | 62.5 |
| | 15 | 404 | 78.7 | 55 | 91 | 0.644 | 64.4 |
| | 20 | 391 | 61.6 | 45 | 107 | 0.721 | 72.1 |
| | 25 | 409 | 54.60 | 70 | 106 | 0.753 | 75.3 |

### 3.3. Electrochemical Impedance Spectroscopy

Impedance diagram (Nyquist) at frequencies ranging from 1 Hz to 1 kHz with 10 mV amplitude signal at OCP for 304SS in 1 M HCl in the absence and presence of different concentrations of compounds are obtained. The equivalent circuit that describes our metal/electrolyte interface is shown in Figure (7) where $R_s$, $R_{ct}$ and CPE refer to solution resistance, charge transfer resistance and constant phase element, respectively. EIS parameters and % IE were calculated and tabulated in Table (7). In order to correlate impedance and polarization methods, $i_{corr}$ values were obtained from polarization curves and Nyquist plots in the absence and presence of different concentrations of investigated compounds using the Stern-Geary equation:

$$i_{corr} = \frac{\beta_a \beta_c}{2.303\,(\beta_a + \beta_c)\,R_{ct}} \qquad (11)$$

The obtained Nyquist plot for compound (1) is shown in Figure (8). Each spectrum is characterized by a single full semicircle. The fact that impedance diagrams have an approximately semicircular appearance shows that the corrosion of 304SS is controlled by a charge transfer process. Small distortion was observed in some diagrams, this distortion has been attributed to frequency dispersion [50]. The diameters of the capacitive loop obtained increases in the presence of organic derivatives, and were indicative of the degree of inhibition of the corrosion process [51].

It was observed from the obtained EIS data that $R_{ct}$ increases and $C_{dl}$ decreases with the increasing of inhibitor concentrations. The increase in $R_{ct}$ values, and consequently of inhibition efficiency, may be due to the gradual replacement of water molecules by the adsorption of the inhibitor molecules on the metal surface to form an

adherent film on the metal surface. This suggests that the coverage of the metal surface by the film decreases the double layer thickness. Also, this decrease of $C_{dl}$ at the metal/solution interface with increasing the inhibitor concentration can result from a decrease in local dielectric constant which indicates that the inhibitors were adsorbed on the surface at both anodic and cathodic sites [52].

The impedance data confirm the inhibition behavior of the inhibitors obtained with other techniques. From the data of Table (7), it can be seen that the $i_{corr}$ values decrease significantly in the presence of these additives and the % IE is greatly improved. The order of reduction in $i_{corr}$ exactly correlates with that obtained from potentiostatic polarization studies. Moreover, the decrease in the values of $i_{corr}$ follows the same order as that obtained for the values of $C_{dl}$. It can be concluded that the inhibition efficiency found from weight loss, polarization curves, electrochemical impedance spectroscopy measurements and the Stern-Geary equation are in good agreement.

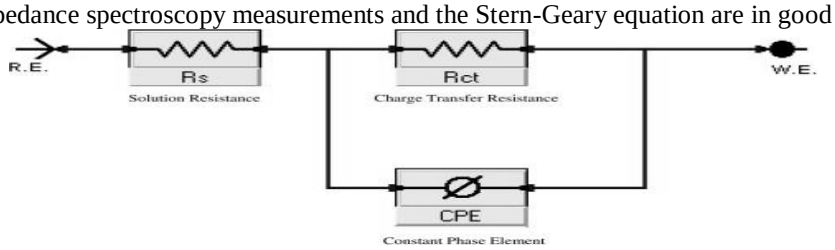


Figure (7): Equivalent circuit model used to fit experimental EIS

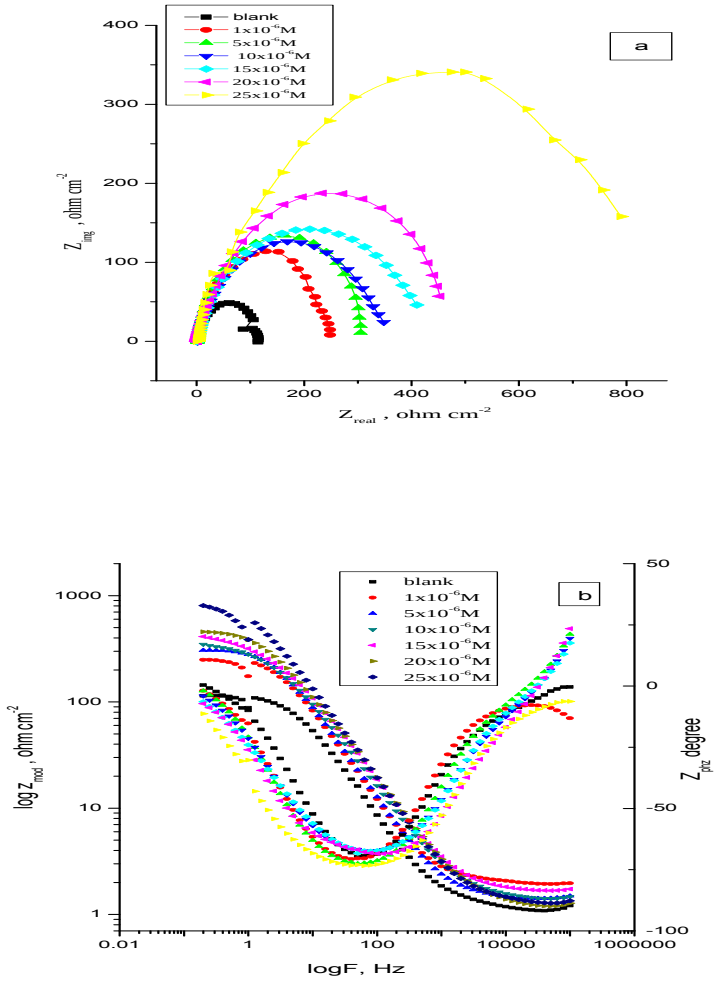


**Figure (8): The Nyquist (a) and Bode (b) plots for corrosion of 304SS in 1 M HCl in the absence and presence of different concentrations of compound (1) at 25°C**

**Table (7): Electrochemical kinetic parameters obtained from EIS technique for 304SS in 1M HCl in the absence and presence of different concentrations of Chalcone compounds at 25°C**

| Comp. | Conc., M | $R_S$, $\Omega\ cm^2$ | $Y_o$, x $10^{-6}$ $\mu\Omega^{-1}s^n$ | n x$10^{-3}$ | $R_{ct}$ $\Omega\ cm^2$ | $C_{dl}$, x$10^4$ $\mu\ Fcm^{-2}$ | θ | %IE |
|---|---|---|---|---|---|---|---|---|
| 1 | Blank | 1.148 | 412.5 | 876.1 | 113.7 | 2.67 | ----- | ------ |
| | 1x$10^{-6}$ | 1.994 | 282.5 | 884.5 | 247.2 | 1.99 | 0.540 | 54.0 |
| | 5x$10^{-6}$ | 1.438 | 262.6 | 888.5 | 290.0 | 1.921 | 0.608 | 60.8 |
| | 10x$10^{-6}$ | 1.427 | 302.2 | 828.8 | 341.5 | 1.89 | 0.667 | 66.7 |
| | 15x$10^{-6}$ | 1.657 | 275.8 | 823.9 | 396.6 | 1.718 | 0.713 | 71.3 |
| | 20x$10^{-6}$ | 1.195 | 265.9 | 823.8 | 486.1 | 1.70 | 0.766 | 76.6 |
| | 25x$10^{-6}$ | 1.444 | 176.7 | 828.7 | 657.1 | 1.13 | 0.827 | 82.7 |
| 2 | 1x$10^{-6}$ | 1.676 | 337.2 | 863.5 | 230.0 | 2.22 | 0.506 | 50.6 |
| | 5x$10^{-6}$ | 1.994 | 282.5 | 884.5 | 270.0 | 1.99 | 0.579 | 57.9 |
| | 10x$10^{-6}$ | 1.727 | 232.5 | 741.5 | 323.2 | 1.9 | 0.648 | 64.8 |
| | 15x$10^{-6}$ | 1.321 | 349.9 | 859.7 | 360.8 | 1.88 | 0.685 | 68.5 |
| | 20x$10^{-6}$ | 1.657 | 275.8 | 823.9 | 396.6 | 1.72 | 0.713 | 71.3 |
| | 25x$10^{-6}$ | 1.608 | 224.9 | 816.6 | 464.0 | 1.70 | 0.755 | 75.5 |

**3.4. Electrochemical Frequency Modulation technique (EFM)**

EFM is a nondestructive corrosion measurement technique that can directly and quickly determine the corrosion current value without prior knowledge of Tafel slopes, and with only a small polarizing signal. These advantages of EFM technique make it an ideal candidate for online corrosion monitoring [53].

The great strength of the EFM is the causality factors which serve as an internal check on the validity of EFM measurement. The causality factors CF-2 and CF-3 are calculated from the frequency spectrum of the current responses. Figure (9) shows the frequency spectrum of the current response of pure 304SS in 1 M HCl, contains not only the input frequencies, but also contains frequency components which are the sum, difference, and multiples of the two input frequencies. The EFM intermodulation spectrums of pure 304SS in 1M HCl acid solution containing (1x$10^{-5}$ M and 25x$10^{-5}$ M) of the studied inhibitors are shown in Figure (9). Similar results were recorded for the other concentrations of the investigated compounds (not shown). The harmonic and intermodulation peaks are clearly visible and are much larger than the background noise. The two large peaks, with amplitude of about 200 µA, are the response to the 40 and 100 mHz (2 and 5 Hz) excitation frequencies. It is important to note that between the peaks there is nearly no current response (<100 nA). The experimental EFM–data were treated using two different models: complete diffusion control of the cathodic reaction and the "activation" model. For the latter, a set of three non-linear equations had been solved, assuming that the corrosion potential does not change due to the polarization of the working electrode [54]. The larger peaks were used to calculate the corrosion current density ($i_{corr}$),

the Tafel slopes ($\beta_c$ and $\beta_a$) and the causality factors (CF-2 and CF-3).These electrochemical parameters were simultaneously determined by Gamry EFM140 software, and listed in Table (8). The data presented in Table (8) obviously show that, the addition of any one of tested compounds at a given concentration to the acidic solution decreases the corrosion current density, indicating that these compounds inhibit the corrosion of 304SS in 1 M HCl through adsorption. The causality factors obtained under different experimental conditions are approximately equal to the theoretical values (2 and 3) indicating that the measured data are verified and of good quality [55]. The inhibition efficiencies %IE $_{EFM}$ increase by increasing the studied inhibitor concentrations and was calculated as follows:

$$\% IE_{EFM} = [(1- i_{corr}/ i^{o}_{corr})] \times 100 \quad (11)$$

where $i^{o}_{corr}$ and $i_{corr}$ are corrosion current densities in the absence and presence of inhibitor, respectively.
The inhibition sufficiency obtained from this method is in the order: compound (1) > compound (2).

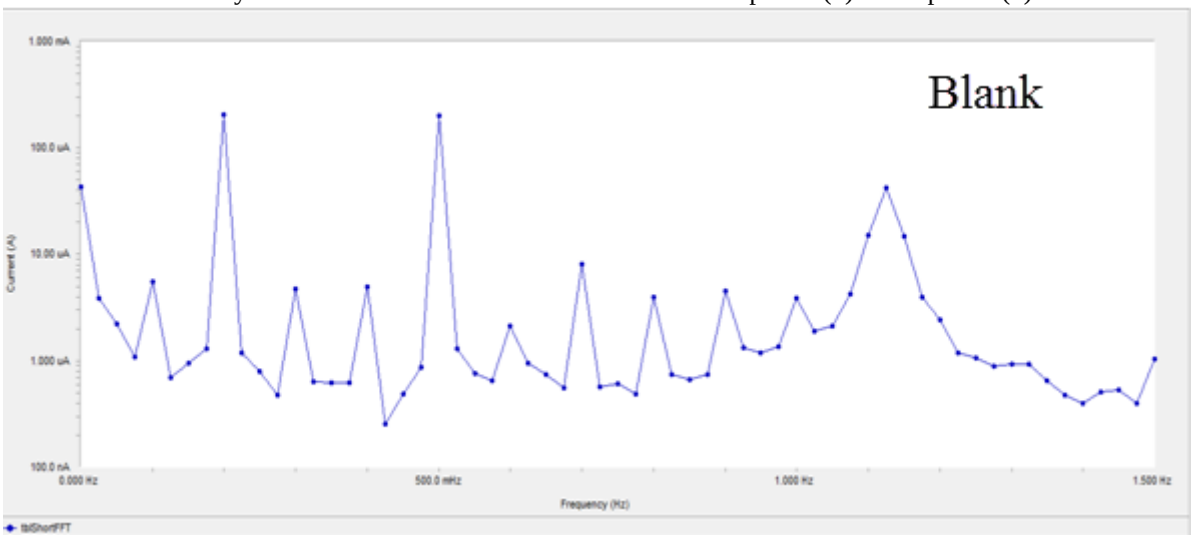


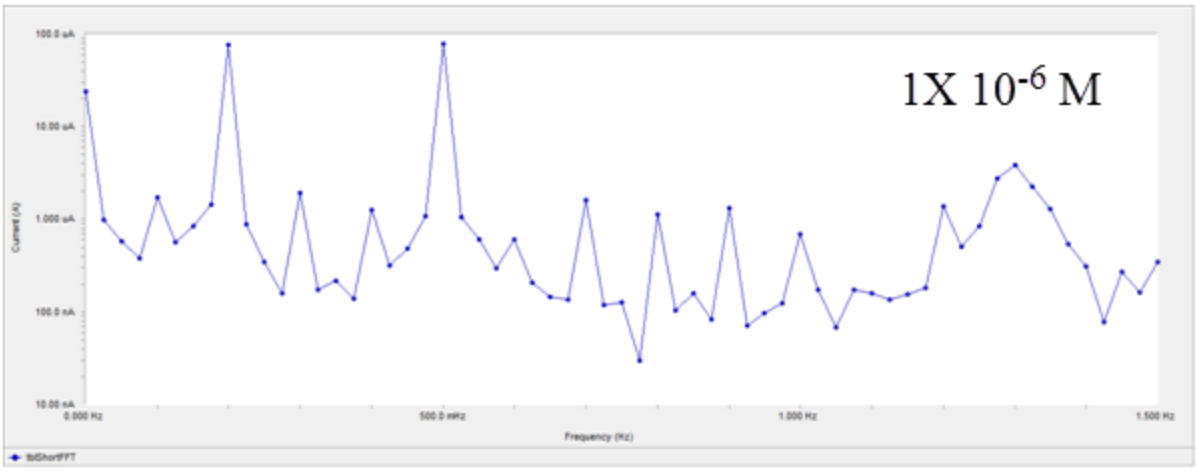

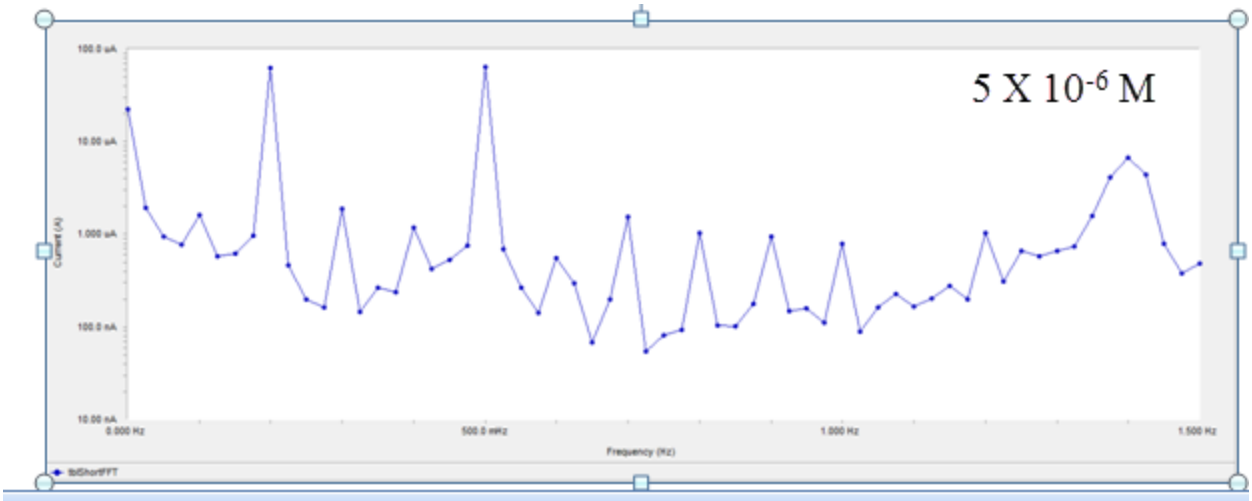
5 X 10-6 M
100.0 uA
10.00 uA
1.000 uA
100.0 nA
10.00 nA
Current (A)
0.000 Hz
500.0 mHz
1.000 Hz
1.500 Hz
Frequency (Hz)
tbiShortFFT

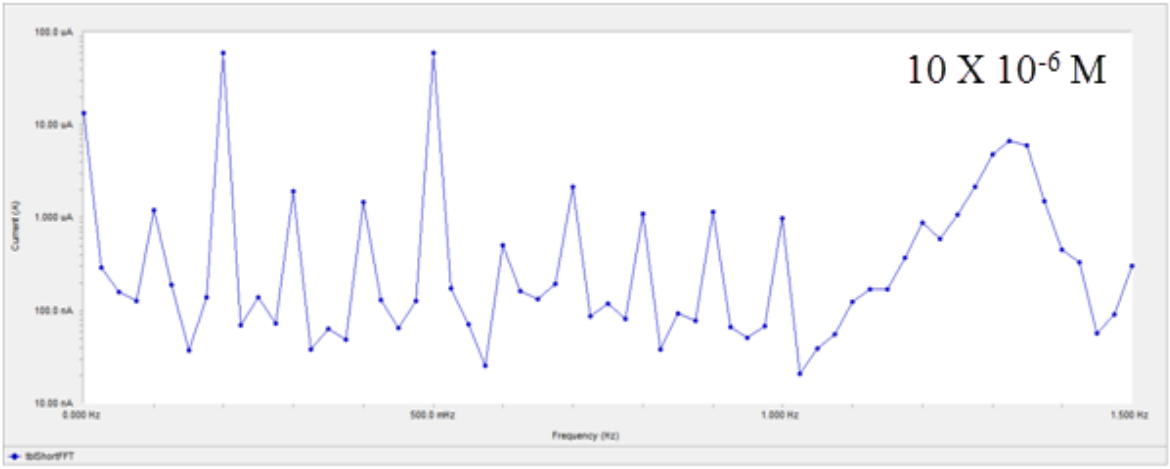
10 X 10-6 M
100.0 uA
10.00 uA
1.000 uA
100.0 nA
10.00 nA
Current (A)
0.000 Hz
500.0 mHz
1.000 Hz
1.500 Hz
Frequency (Hz)
tbiShortFFT

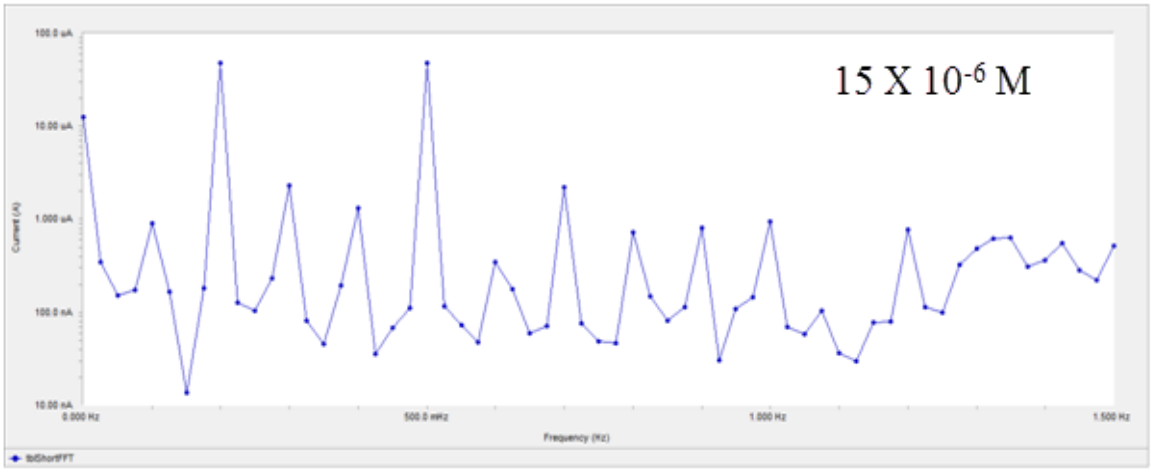
15 X 10-6 M
100.0 uA
10.00 uA
1.000 uA
100.0 nA
10.00 nA
Current (A)
0.000 Hz
500.0 mHz
1.000 Hz
1.500 Hz
Frequency (Hz)
tbiShortFFT

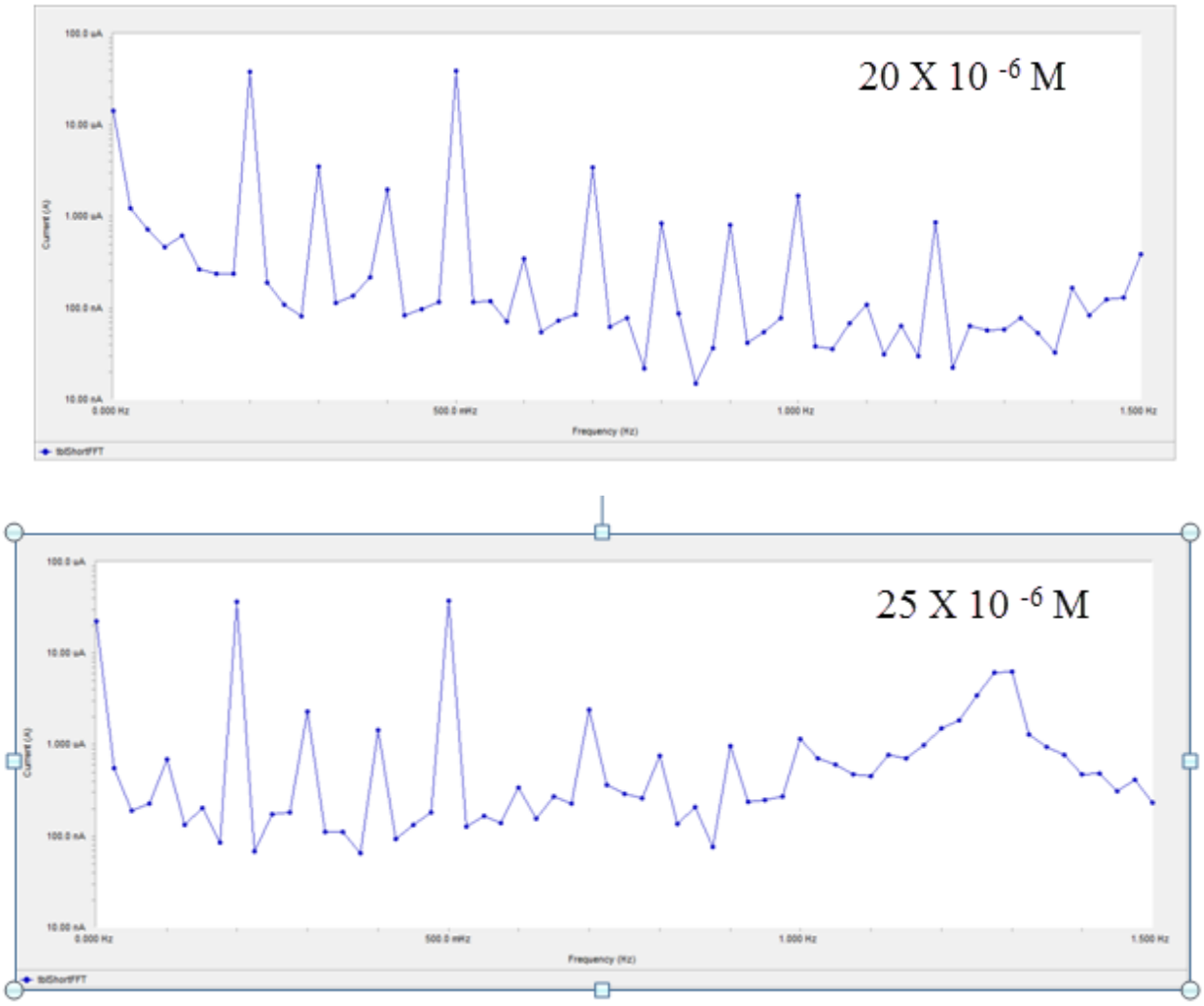


**Figure (9): EFM spectra for SS type 304 in 1 M HCl in thepresence and absence of different concentrations of compond (1) at 25˚C**

**Table (8): Electrochemical kinetic parameters obtained from EFM technique for 304SS in 1 M HCl in the absence and presence of different concentrations of Chalcone compounds at 25°C**

| Comp. | Conc., M | $i_{corr}$ µAcm$^{-2}$ | $\beta_c$ mVdec$^{-1}$ | $\beta_a$ mVdec$^{-1}$ | CF-2 | CF-3 | CR mpy | θ | %IE |
|---|---|---|---|---|---|---|---|---|---|
| | Blank | 253.2 | 88 | 75 | 1.9 | 2.9 | 115.7 | - | - |
| 1 | 1x10$^{-6}$ | 102.8 | 92 | 81 | 2.0 | 2.8 | 46.9 | 0.594 | 59.4 |
| | 5x10$^{-6}$ | 82.93 | 92 | 80 | 1.9 | 2.9 | 37.9 | 0.672 | 67.2 |
| | 10x10$^{-6}$ | 79.57 | 95 | 79 | 1.8 | 2.8 | 36.3 | 0.685 | 68.5 |
| | 15x10$^{-6}$ | 67.49 | 105 | 81 | 2.0 | 2.7 | 30.8 | 0.733 | 73.3 |

| | | | | | | | | | |
|---|---|---|---|---|---|---|---|---|---|
| | $20x10^{-6}$ | 51.76 | 115 | 70 | 2.0 | 2.7 | 23.6 | 0.795 | 79.5 |
| | $25x10^{-6}$ | 41.93 | 86 | 64 | 2.1 | 2.8 | 19.1 | 0.834 | 83.4 |
| 2 | $1x10^{-6}$ | 134.4 | 88 | 78 | 2.1 | 2.8 | 74.6 | 0.530 | 53.0 |
| | $5x10^{-6}$ | 103.7 | 92 | 76 | 2.1 | 2.7 | 47.4 | 0.590 | 59.0 |
| | $10x10^{-6}$ | 92.42 | 98 | 75 | 2.0 | 2.9 | 42.2 | 0.635 | 63.5 |
| | $15x10^{-6}$ | 81.49 | 95 | 80 | 2.0 | 3.0 | 37.2 | 0.678 | 67.8 |
| | $20x10^{-6}$ | 63.63 | 111 | 86 | 1.9 | 2.9 | 29.0 | 0.748 | 74.8 |
| | $25x10^{-6}$ | 53.31 | 151 | 83 | 1.9 | 2.9 | 24.3 | 0.789 | 78.9 |

***3.5- Scanning Electron Microscopy (SEM) Studies***

Figure (10) represents the micrography obtained for 304SS samples in presence and in absence of 25 x $10^{-5}$ M Chalcone derivatives compounds after exposure for 3 days immersion. It is clear that 304SS surfaces suffer from severe corrosion attack in the blank sample. It is important to stress out that when the compound is present in the solution, the morphology of 304SS surfaces is quite different from the previous one, and the specimen surfaces were smoother. We noted the formation of a film which is distributed in a random way on the whole surface of the 304SS. This may be interpreted as due to the adsorption of the Chalcone compounds on the 304SS surface incorporating into the passive film in order to block the active site present on the carbon steel surface. Or due to the involvement of inhibitor molecules in the interaction with the reaction sites of 304SS surface, resulting in a decrease in the contact between carbon steel and the aggressive medium and sequentially exhibited excellent inhibition effect [56,57].

Pure sample Blank

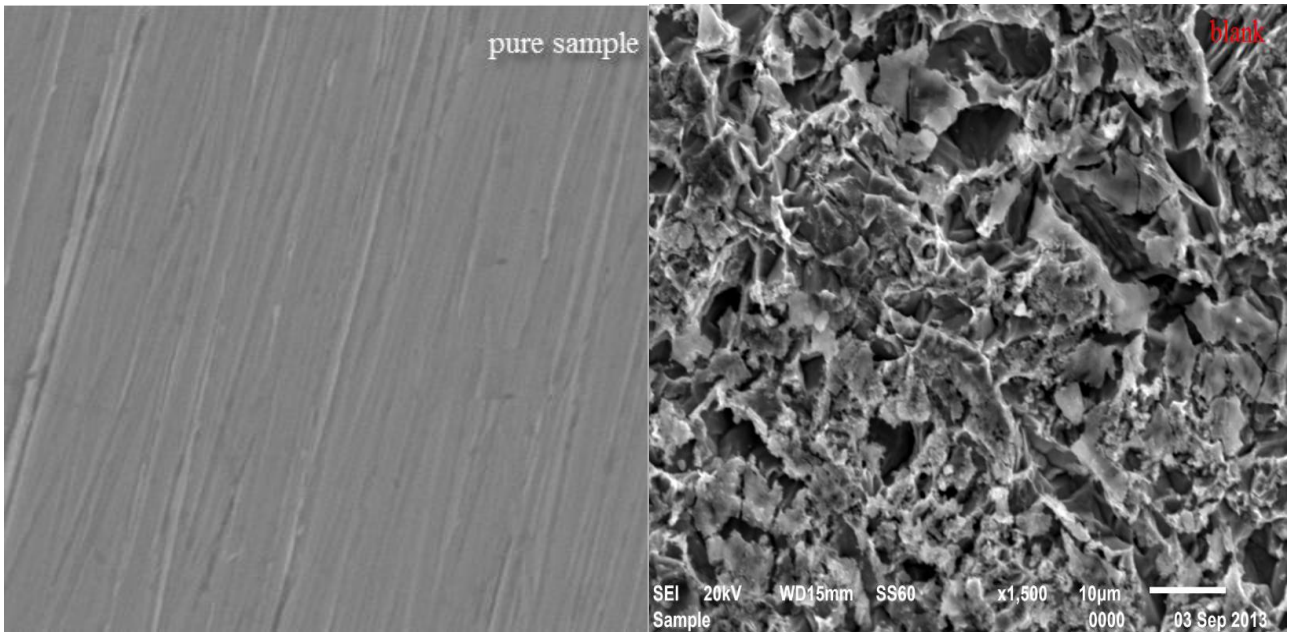

Compond (1) Compond (2)

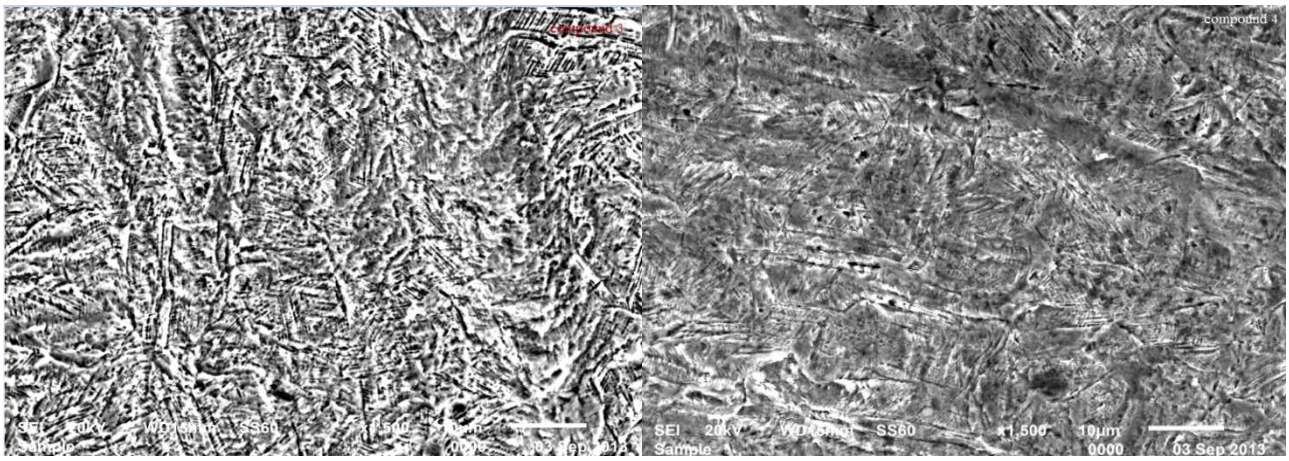

**Figure (10): SEM micrographs for SS type 304in absence and presence of $25x10^{-5}$ M of chalcone compounds**

***3.6. Energy Dispersive X-ray Spectroscopy (EDX) Studies***

The EDX spectra were used to determine the elements present on the surface of 304SS and after 3 days of exposure in the uninhibited and inhibited 1M HCl. Figure (11) shows the EDX analysis result on the composition of 304SS only without the acid and inhibitor treatment. The EDX analysis indicates that only Fe and oxygen were detected, which shows that the passive film contained only $Fe_2O_3$

Figure (11) portrays the EDX analysis of 304SS in 1 M HCl only and in the presence of $25x10^{-5}$ M of Chalcone compounds. The spectra show additional lines, demonstrating the existence of C (owing to the carbon atoms of Chalcone compounds). These data shows that the carbon and O atoms covered the specimen surface. This layer is entirely owing to the inhibitor, because the carbon and O signals are absent on the specimen surface exposed to uninhibited HCl. It is seen that, in addition to Mn, C. and O were present in the spectra. A comparable elemental distribution is shown in Table (9).

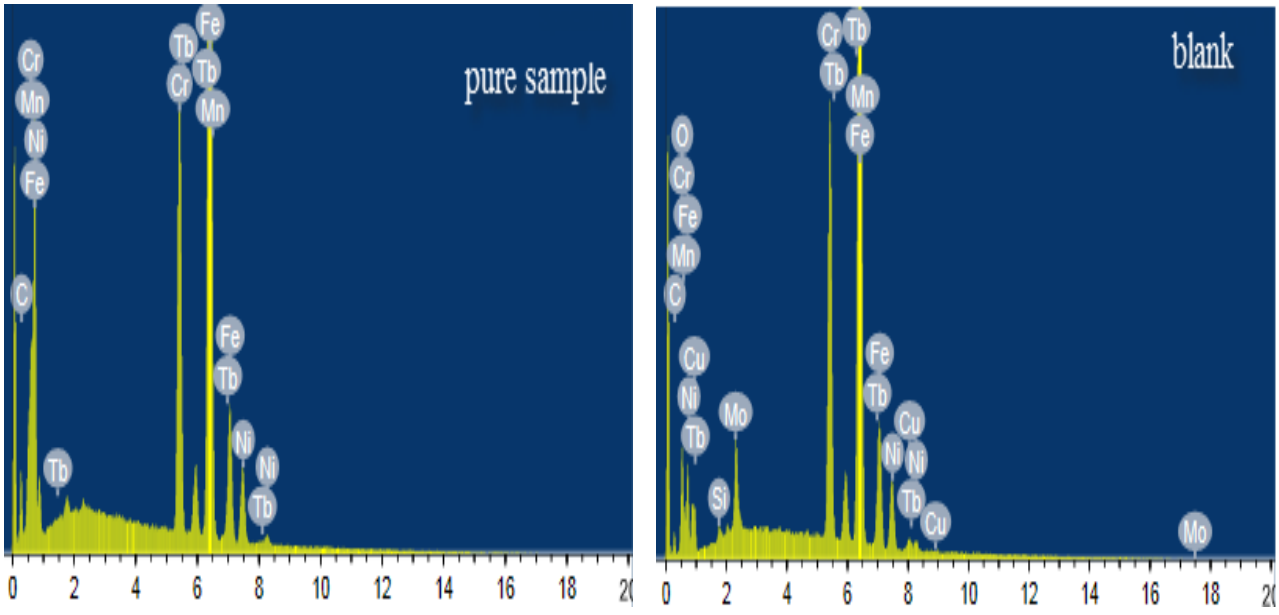

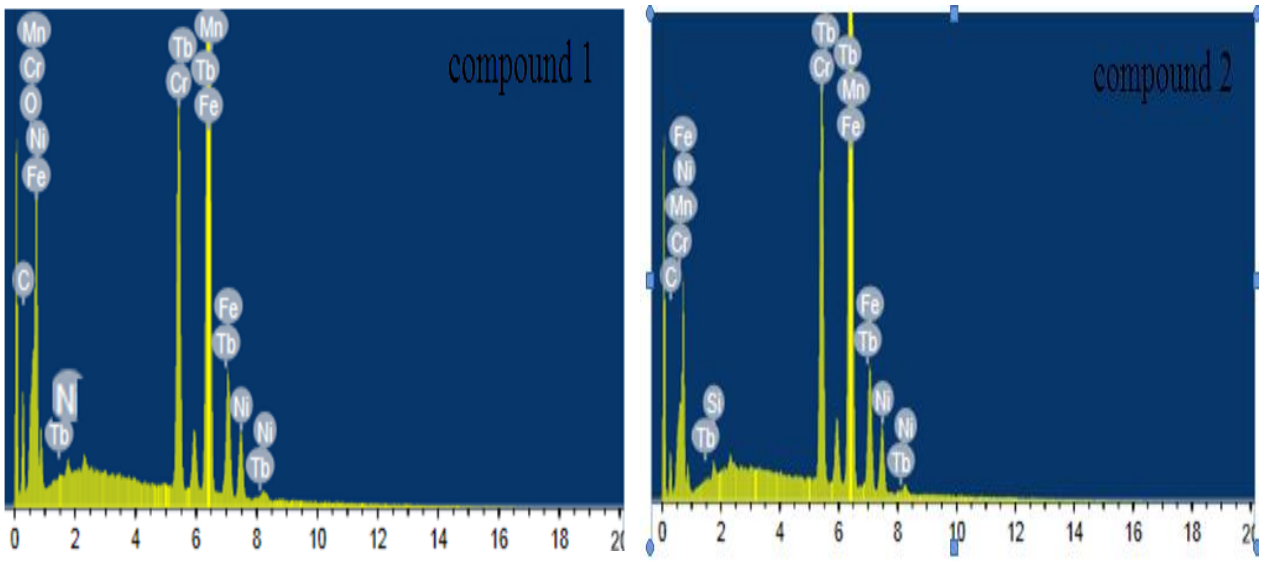


**Figure. (11): EDX analysis for 304SS absence and presence of $25x10^{-5}$ M of Chalcone compounds for 3 days immersion**

**Table (9): Surface composition (weight %) of 304SS after 3days of immersion in 1 HCl without and with the optimum concentrations of the studied inhibitors**

| (Mass %) | Fe | Mn | C | O | Cr | S | N | Tb |
|---|---|---|---|---|---|---|---|---|
| Pure | 60.62 | 1.10 | 9.91 | ---- | 16.78 | ---- | ---- | 7.23 |
| Blank | 52.06 | 0.81 | 0.65 | 1.56 | 15.48 | ----- | ----- | ---- |
| Compound (1) | 55.87 | 0.86 | 9.63 | 3.94 | 13.99 | ---- | 6.03 | 6.52 |
| Compound (2) | 55.37 | 0.78 | 9.27 | 2.14 | 12.73 | ---- | ---- | 6.53 |

### *3.7. Quantum chemical calculations*

Theoretical calculations were performed for only the neutral forms, in order to give further insight into the experimental results. Values of quantum chemical indices such as energies of LUMO and HOMO ($E_{HOMO}$ and $E_{LUMO}$), the formation heat $\Delta H_f$ and energy gap $\Delta E$, are calculated by semi-empirical AM1, MNDO and PM3 methods has been given in Table(10).The reactive ability of the inhibitor is related to $E_{HOMO}$, $E_{LUMO}$[58]. Higher $E_{HOMO}$ of the adsorbent leads to higher electron donating ability. Low $E_{LUMO}$ indicates that the acceptor accepts electrons easily. The calculated quantum chemical indices ($E_{HOMO}$, $E_{LUMO}$, μ) of investigated compounds are shown

in Table (10). The difference $\Delta E = E_{LUMO} - E_{HOMO}$ is the energy required to move an electron from HOMO to LUMO. Low ΔE facilities adsorption of the molecule and thus will cause higher inhibition efficiency. The bond gap energy ΔE increases from (1 to 2). This fact explains the decreasing inhibition efficiency in this order (1>2), as shown in Table (10) and Figure (12) show the optimized structures of the three investigated compounds. So, the calculated energy gaps show reasonably good correlation with the efficiency of corrosion inhibition. Table (10) also indicates that compound (1) possesses the lowest total energy that means that compound (1) adsorption occurs easily and is favored by the highest softness. The HOMO and LUMO electronic density distributions of these molecules were plotted in Figure (12). For the HOMO of the studied compounds that the benzene ring, N-atoms and O-atom have a large electron density. The data presented in Table (8) show that the calculated dipole moment decrease from compound (1) > compound (2).

| Structure | HOMO | LUMO | Mulliken charges |
|---|---|---|---|
| 1 | 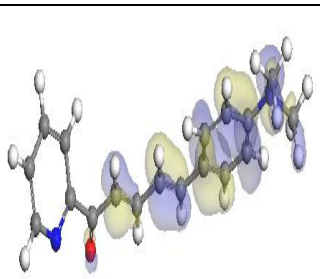 | 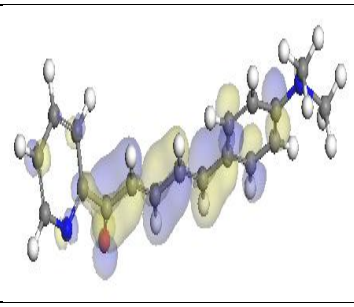 | 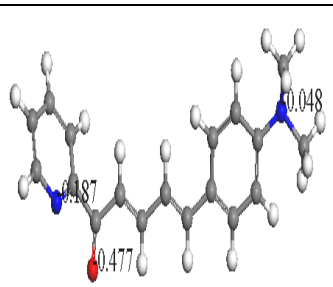  |
| 2 | 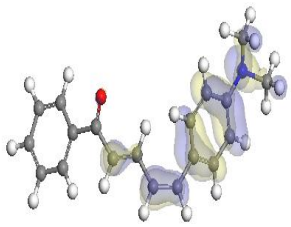 | 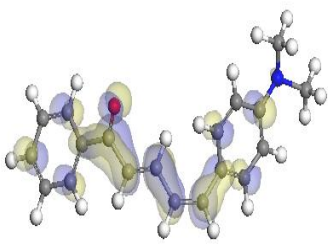 | 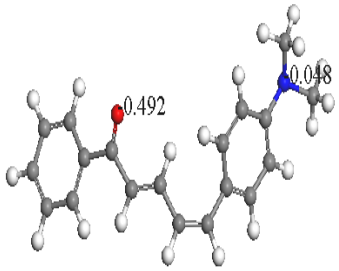  |

**Figure (12): Molecular orbital plots and Mulliken charges of organic compounds**

**Table (10): The calculated quantum chemical parameters for investigated compounds by using PM3**

| | Compound (1) | Compound (2) |
|---|---|---|
| $-E_{HOMO}$ ( eV) | 8.656 | 8.717 |
| $-E_{LUMO}$ (eV) | 1.294 | 1.145 |
| ΔE (eV) | 7.362 | 7.572 |
| Dipole moment, μ , (Debye) | 6.751 | 3.725 |
| Molecular Area ($Å^2$) | 330.429 | 329.331 |

### 3.8- Chemical Structure of the Inhibitors and Corrosion Inhibition

Inhibition of the corrosion of 304SS in 1M HCl solution by some Chalcone compounds is determined by weight loss, potentiodynamic anodic polarization measurements, Electrochemical Impedance Spectroscopy (EIS), electrochemical frequency modulation method (EFM) and Scanning Electron Microscopy (SEM) Studies, it was found that the inhibition efficiency depends on concentration, nature of metal, the mode of adsorption of the inhibitors and surface conditions. The observed corrosion data in presence of these inhibitors, namely: i) The decrease of corrosion rate and corrosion current with increase in concentration of the inhibitor, ii) The linear variation of weight loss with time, iii) The shift in Tafel lines to higher potential regions, iv) The decrease in corrosion inhibition with increasing temperature indicates that desorption of the adsorbed inhibitor molecules takes

place and v) The inhibition efficiency was shown to depend on the number of adsorption active centers in the molecule and their charge density.

It was concluded that the mode of adsorption depends on the affinity of the metal towards the π-electron clouds of the ring system. Metals such as Cu and Fe, which have a greater affinity towards aromatic moieties, were found to adsorb benzene rings in a flat orientation. The order of decreasing the percentage inhibition efficiency of the investigated inhibitors in the corrosive solution was as follow: compound (1) > compound (2)
Compound (1) exhibits excellent inhibition power due to: (i) its larger molecular size that may facilitate better surface coverage, and (ii) its adsorption through one oxygen atom and two nitrogen atoms. Compound (2) comes after compound (1) in inhibition efficiency due to its lower molecular size than compound (1) and it contains one oxygen atom and only one nitrogen atom.

4. References

[1] H. Keles, M. Keles, I. Dehri, O. Serindag. Mater. Chem. Phys.112 (2008) 173.
[2] H. Wang, H. Fan, J. Zheng. Mater. Chem. Phys. 77 (2003)655.
[3] S.A.A. El-Maksoud, A.S. Fouda. Mater. Chem. Phys. 93 (2005) 84.
[4] M. Lagrenee, B. Mernari, M. Bouanis, M. Traisnel, F. Bentiss.Corros. Sci. 44 (2002) 573.
[5] M. Abdallah. Corros. Sci. 45 (2003) 2705.
[6] I.B. Obot, N.O. Obi-Egbedi. Corros. Sci. 52 (2010) 657.
[7] Y. Tang, X. Yang, W. Yang, R. Wan, Y. Chen, X. Yin.Corros. Sci. 52 (2010) 1801.
[8] L. Wang. Corros. Sci. 43 (2001) 2281.
[9] A. Popova, M. Christov, T. Deligeorgiev.Corrosion 59 (2003) 756.
[10] K.F. Khaled. Electrochim. Acta 48 (2003) 2493.
[11] X. Wang, H. Yang, F. Wang.Corros. Sci. 53 (2011) 113.
[12] A. Popova, E. Sokolova, S. Raicheva, M. Christov. Corros. Sci. 45 (2003) 33.
[13] A. Popova, M. Christov, S. Raicheva, E. Sokolova. Corros.Sci. 46 (2004) 1333.
[14] M. Christov, A. Popova, . Corros. Sci. 46 (2004) 1613.
[15] A. Popova, M. Christov, A. Zwetanova.Corros. Sci. 49 (2007) 2131.
[16] A. Popova, M. Christov, A. Vasilev.Corros. Sci. 49 (2007) 3290.
[17] I. Ahamad, M.A. Quraishi, Mebendazole. Corros. Sci. 52 (2010) 651.
[18] I. Ahamad, M.A. .Corros. Sci. 51(2009) 2006.
[19] N. Khalil. Electrochim.Acta 48 (2003) 2635.
[20] E.S.H.E. Ashry, A.E. Nemr, S.A. Esawy, S. Ragab. Electrochim.Acta 51 (2006) 3957.
[21] R. Hasanov, M. Sadıkog˘lu, S. Bilgic. Appl.Surf. Sci. 253 (2007) 3913.
[22] M. Ozcan, _I. Dehri Prog. Org. Coat. 51 (2004) 181.
[23] Y. Xiao-Ci, Z. Hong, L. Ming-Dao, R. Hong-Xuan, Y. Lu-An,Corros. Sci. 42 (2000) 645.
[24] I.B. Obot, N.O. Obi-Egbedi. Colloids Surf., A 330 (2008) 207.
[25] I.B. Obot, N.O. Obi-Egbedi. Surf. Rev. Lett. 15 (2008) 903.
[26] I.B. Obot, N.O. Obi-Egbedi, S.A. Umoren. Corros. Sci. 51(2009)276.
[27] K.F. Khaled.Electrochim.Acta 53 (2008) 3484.
[28] E.E. Oguzie, C.K. Enenebeaku, C.O. Akalezi, S.C. Okoro, A.A. Ayuk, E.N. Ejike.J. Colloid Interface Sci. 349 (2010) 283.
[29] J. Zhou, S. Chen, L. Zhang, Y. Feng, H. Zhai.J. Electroanal. Chem.612 (2008) 257.
[30] K.F. Khaled, M.A. Amin, . Corros. Sci. 51 (2009) 1964.
[31] Y. Tang, L. Yao, C. Kong, W. Yang, Y. Chen. Corros. Sci. 53(2011) 2046.
[32] K.F. Khaled.Electrochim. Acta 54 (2009) 4345.
[33] J. Zhang, Q. Zhang, H. Ren, W. Zhao, H. Zhang. Appl. Surf. Sci.253 (2007) 7416.
[34] S. Xia, M. Qiu, L. Yu, F. Liu, H. Zhao. Corros. Sci. 50 (2008) 2021.

[35] J.D.Talati and R.M.Modi, Trans.SEAST, 11 (1986) 259.
[36]R. W. Bosch, J. Hubrecht, W. F. Bogaerts, B. C. Syrett, *Corrosion* 57 (2001) 60.
[37]S. S. Abdel–Rehim, K. F. Khaled, N. S. Abd–Elshafi, *Electrochim. Acta*51 (2006) 3269.
[38] Tomasz Tronina, AgnieszkaBartmańska, BeataFilip-Psurska, Joanna Wietrzyk, JarosławPopłoński, EwaHuszczaBioorganic& Medicinal Chemistry*21* (7) (2013) 2001.

[39] Z.Szklarska-Smiaiowska; Electrochemical and Optical Techniques for the Study of Metallic Corrosion, Kluwer Academic, the Netherlands; (1991) 545.

[40] I.Langmuir, J.Amer.Chem.Soc., 39 (1947) 1848.

[41] E.Khamis, Corrosion, 46 (1990) 476.

[42] G. Trabanelli, in "Corrosion Mechanisms" (Ed. F. Mansfeld) Marcel Dekker, New York,

119 (1987).

[43] F.H. Asaf, M. Abou- Krisha, M. Khodari, F. EL-Cheihk, A. A. Hussien, Mater Chem. Phys., 93 (2002) 1.

[44] A.Fiala, A. Chibani, A. Darchen, A. Boulkamh, K. Djebbar, Appl. Surf. Sci. 253

(2007) 9347.

[45] S.T. Arab and E.M. Noor, Corrosion 49 (1993) 122.

[46] W. Durnie, R.D. Marco, A. Jefferson, B. Kinsella, J. Electrochem. Soc., 146 (1999) 1751.

[47] J. M. Thomas and W. J. Thomas, Introduction to the Principles of Heterogeneous Catalysis, 5th Ed, Academic Press, London (1981) 14.

[48] A. El-Ouafi, B. Hammouti, H. Oudda, S. Kerit, R. Touzani, A. Ramdani, *Anti-Corros. Meth.Mater.*49 (2002) 199.

[49]F. Mansfeld, M.W. Kendig, S. Tsai, *Corrosion*, 38 (1982) 570.

[50] F. Mansfeld, *Eletrochim. Acta*, 35 (1990) 1533.

[51]E. McCafferty, N Hackerman, *J. Electrochem. Soc.* 119 (1972) 146.

[52] E. Kus, F. Mansfeld, *Corros. Sci.* 48 (2006) 965.

[53] G. A. Caigman, S. K. Metcalf, E. M. Holt, *J.Chem. Cryst*.30 (2000) 415.

[54] D.C. Silverman and J.E. Carrico, *National Association of Corrosion Engineers*, 44 (1988), 280.

[55] R.A., Prabhu, T.V., Venkatesha, A.V., Shanbhag, G.M., Kulkarni, R.G., Kalkhambkar,*Corros.Sci.*, 50 (2008) 3356

[56] G., Moretti, G., Quartanone, A., Tassan, A., Zingales, ,*Wekst. Korros.*,45(1994) 641

[57] C. Lee, W. Yang and R. G. Parr., *Phys. Rev. B*, 37 (1988) 785.

[58] R. M. Issa, M. K. Awad and F. M. Atlam, *Appl. Surf. Sci.*, 255 (2008) 2433